

# First-principles Calculations of Engineered Surface Spin Structures

Chiung-Yuan Lin<sup>1</sup> and B. A. Jones<sup>2</sup>

<sup>1</sup>*Department of Electronics Engineering, National Chiao Tung University, Hsinchu, Taiwan*

<sup>2</sup>*IBM Almaden Research Center, San Jose, CA 95120-6099, USA*

(Dated: April 2, 2024)

The engineered spin structures recently built and measured in scanning tunneling microscope experiments are calculated using density functional theory. By determining the precise local structure around the surface impurities, we find the Mn atoms can form molecular structures with the binding surface, behaving like surface molecular magnets. The spin structures are confirmed to be antiferromagnetic, and the exchange couplings are calculated within 8% of the experimental values simply by collinear-spin GGA+U calculations. We can also explain why the exchange couplings significantly change with different impurity binding sites from the determined local structure. The bond polarity is studied by calculating the atomic charges with and without the Mn adatoms. In addition, we study a second adatom, Co. We study the surface Kondo effect of Co by calculating the surrounding local density of states and the on-site Coulomb  $U$ , and compare and contrast the behavior of Co and Mn. Finally, our calculations confirm that the Mn and Co spins of these structures are  $5/2$  and  $3/2$  respectively, as also measured indirectly by STM.

PACS numbers:

## I. INTRODUCTION

Assembling and manipulating a few spins ( $1\sim 20$ ) is essential for the development of nano magnetic devices. During the past decades, chemists have been able to synthesize molecular magnets that carry giant molecular spins. Potential applications of molecular magnets have been extensively proposed in the literature<sup>1</sup>, such as magnetic storage bits, quantum computation, and magneto-optical switches. The atoms within a molecular magnet form chemical bonds with each other, and therefore are very difficult to manipulate. Instead of assembling atomic spins chemically to form isolated molecules, the advance of manipulating atoms on surfaces by scanning tunnelling microscope (STM) has made it possible to make, probe, and manipulate individual atomic spins.

In a pioneering experiment, Hirjibehedin et al.<sup>2</sup> carried out low-temperature STM measurements of atomic chains of up to 10 Mn atoms. These magnetic chains are assembled by atomic manipulation on copper nitride islands that provide an insulating monolayer between the chains and a Cu(100) substrate (to be called CuN surface later in this paper). Ref. 2 shows the calculation of exchange coupling  $J$  using the Heisenberg Hamiltonian to be successful. It demonstrated that the exchange coupling  $J$  can be tuned by placing the magnetic atoms at different binding sites on the substrate. Nevertheless, the STM experiments can not provide either a detailed study of the single CuN layer or the sub-atomic spatial structures around the Mn atoms. As we will show in this work<sup>3</sup>, the former can explain why tunnelling current and spin can both be preserved, and the later is essential for realizing the molecular magnetism of the Mn-surface complex as well as understanding how  $J$  depends on the Mn binding site. Moreover, the  $5/2$  spin of the Mn atoms on such a CuN surface is calculated directly here rather than indirectly extracting

from inelastic-tunnelling-spectroscopy steps in the experiments.

In addition to the interatomic magnetic coupling, the surface Kondo effect is also an interesting topic in engineered spin systems. Recent studies show that the surface Kondo effect is interestingly influenced by either the magnetic anisotropy of the Kondo atom itself<sup>4</sup> or by being coupled to a second magnetic atom<sup>5</sup>. These systems both have Co as the adatom for their Kondo impurity and are built on the CuN surface that was previously used to study coupling of Mn atoms. These experimental studies explain surface Kondo under external influences using phenomenological models, and obtain great success. However, detailed microscopic understandings such as the local density of states (LDOS) around the Co and the on-site Coulomb repulsion  $U$  were not achieved yet. Also, Ref. 4 concludes indirectly that the Co spin on this surface is  $S = 3/2$  by first excluding  $S = 1/2$  and integer  $S$  from the experimental fitting and then excluding  $S \geq 5/2$  based on the experience that the spins of surface-adsorbed atoms are generally unchanged or reduced from the free atom. Yet a direct measurement or calculation was not done.

In this work, we perform first-principles calculations of the clean CuN surface and of Mn and Co adatoms on this surface with structure optimization. We find, surprisingly, that when the Mn atoms are deposited on the Cu sites of the CuN surface, the nearby N atoms break bounds with their neighboring Cu and form a “quasi” molecular structure on the surface, a situation which does not happen for Mn at the N sites. This fact itself was not determined from experiment, and can only be realized from a first-principles calculation. As a comparison, we study the clean CuN surface and find that the CuN monolayer is formed by polar covalently bounded Cu and N, and such a layer is shown to provide a semi-metal surface layer on the underlying Cu substrate allowing the

coexistence of the Mn spin and STM current. We also accurately calculate the exchange coupling  $J$  using the GGA+ $U$  method, from which we demonstrate that first-principles calculation has the capability of predicting  $J$  of given physical systems. For a Co atom on the same surface, we determined the on-site Coulomb  $U$  that is very important in understanding the Kondo effect. We also compare the LDOS of Co on the Cu and N sites, and explain why the Kondo effect is observed in the experiments on the Cu site but not on the N. Finally, we determine, by analyzing the Co density of states, a Co spin that matches what was measured indirectly from STM experiments<sup>4</sup>.

## II. THEORY

The CuN monolayer between the magnetic atoms and Cu substrate originates from the idea of preserving the atomic spins from being screened by the underlying conduction electrons, while at the same time allowing enough tunneling current from an STM tip to probe the spin excitations. To understand this further in a microscopic picture, we simulate both the Cu(100) and CuN surfaces by a supercell of 7-layer slabs separated by 8 vacuum layers, where for the CuN surface, each slab has CuN monolayers on both sides and three Cu layers in between. The electronic structure is calculated, in the frame work of density functional theory, using the all-electron full-potential linearized augmented plane wave (FLAPW) method<sup>6</sup> with the exchange-correlation potential in the generalized gradient approximation (GGA)<sup>7</sup>. We calculate the LDOS of both the Cu(100) and CuN surfaces at the Fermi energy as a function along the  $z$  direction through the surface Cu atom. As seen from Fig. 1, the LDOS of the clean Cu(100) surface has a much longer tail into vacuum than the CuN surface. The calculated work functions are 4.6 and 5.2 eV respectively, a difference of 0.6 eV, much smaller than a typical bulk insulator, which has a work function  $\gtrsim 3$  eV more than copper. This shows that the CuN monolayer provides the Cu substrate a moderate conduction that makes possible the coexistence of the atomic spin and STM current.

To calculate the electronic structures of Mn(Co) on the CuN surface, we simulate the single magnetic atom on this surface by a supercell of 5-layer slabs similar to the one for CuN surface with the Mn(Co) atoms placed on top of the CuN surface at 7.24 separation. The crystal structure is optimized until the maximum force among all the atoms reduces to  $\lesssim 2$  mRy/ $a_0$ . The 3d orbital can in general have strong Coulomb repulsion  $U$  that can not be taken into account by GGA. Using a constraint-GGA method<sup>8</sup>, we obtain the  $U$  value of a single Mn at the Cu site of the CuN surface to be 4.9 eV, and 3.9 eV at the N site. Since the calculated Mn  $U$ 's fall in the range of strong correlation, they are then used in the GGA+ $U$  calculation<sup>10</sup> for Mn 3d. To calculate a Mn dimer on the CuN surface, we simulate the system by the same

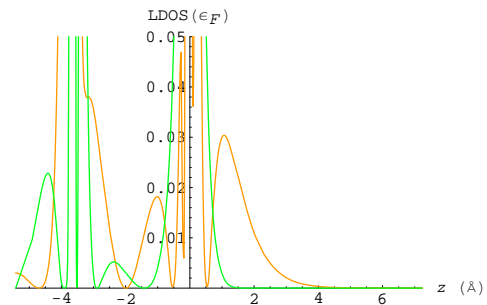


Figure 1: LDOS( $\epsilon_F$ ) along the out-of-surface direction with the surface Cu atom as the origin, for both the clean Cu(100) (orange) and CuN (green) surfaces. (The vacuum corresponds to positive values of  $z$ .)

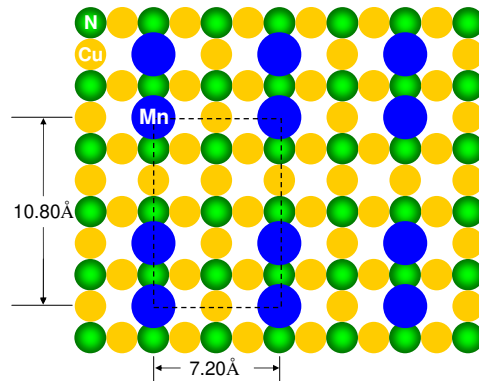


Figure 2: Unit cell of a Mn dimer on the CuN surface.

slab setup as the single Mn except that the Mn atoms on the surface are arranged as in Fig. 2. The electronic structure is also calculated using GGA+ $U$  with  $U$  on the Mn 3d orbitals. For Co on the Cu site, we also apply the constraint-GGA method and obtain  $U = 0.8$  eV. We then calculate this system by GGA with no additional  $U$ . In fact, since the experiments show such a Co adatom exhibits the Kondo effect, it does not make sense to apply the  $U$  statically in a dynamical process (Kondo).

## III. RESULTS AND DISCUSSION

To see the effect on the surface of the presence of Mn atoms, we plot the electron density of the clean CuN surface in Fig. 3. We find the N atoms snug in between the surface Cu atoms to form a CuN surface layer, joined by shared charge densities as well as proximity. The vertical distance between N and the surface Cu is only 0.26 Å, essentially collinear. The density contour shared by N and Cu indicates that a polar covalent bond is formed



Figure 3: Electron density contour of the CuN surface along the N row and the out-of-plane direction.

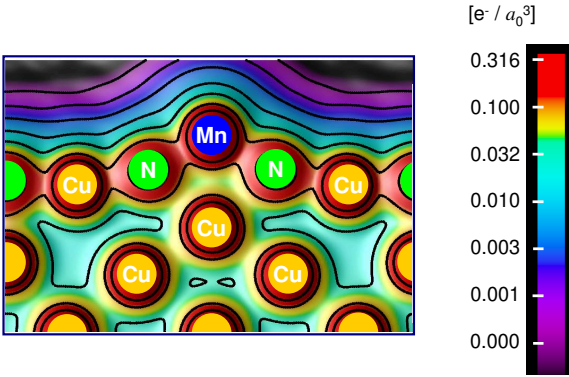


Figure 4: Electron density contour of a single Mn on the CuN surface along the N-Mn-N row and the out-of-plane direction.

between Cu (metallic) to N (larger electronegativity). In fact, a Bader analysis<sup>9</sup> on our calculated electron-density distribution shows N and surface Cu are  $-1.2$  and  $+0.6$  charged respectively. Fig. 4 shows the electron density contour of a single Mn atom placed on the Cu atom on this surface. As one can see, the atomic structure is substantially rearranged. The Mn atom attracts its neigh-

Exchange coupling $J$ (meV)	Cu-site Mn dimer	Cu-site Mn dimer
GGA+U (calculated $U$ )	$6.50 \pm 0.05$ ( $U = 4.9\text{eV}$ )	2.5 ( $U = 3.9\text{eV}$ )
STM	$6.2 \pm 0.3$	2.7
GGA	18.5	-1.8
GGA+U (calculated $U+1\text{eV}$ )	5.4	5.1

Table I: Calculated exchange coupling  $J$  at different  $U$  values, compared with the STM measurements.

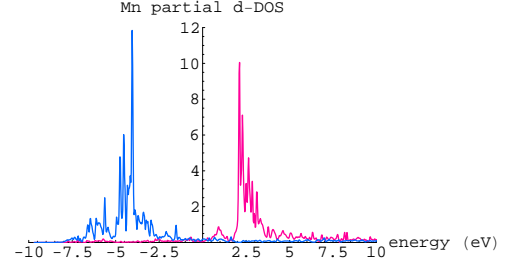


Figure 5: Mn  $d$ -projected density of states of a single Mn on the CuN surface (the leftmost curve (blue in color) for spin up and the rightmost curve (pink) for spin down).

boring N atoms remarkably out of the surface, forming a new polar covalent bond that replaces the CuN binding network, and the Cu atom underneath Mn moves towards the bulk. We have calculated that Mn and its neighboring N are  $+1.0$  and  $-1.3$  charged respectively, indicating that the Mn-N bond has a stronger polarity than the Cu-N.

The calculated density of states for a single Mn on the CuN surface is plotted in Fig. 5. It is clearly seen that the Mn  $3d$  majority spin states are all below the Fermi level and the minority states are all above, which implies a  $3d^5$  configuration for Mn, a spin  $S = 5/2$  configuration. We also do the same analysis for Mn at the N site of the CuN surface, and this structure exhibits the same unchanged Mn spin. This verifies the same conclusion drawn from comparing spin chains of different lengths in the STM experiment<sup>2</sup>.

We now consider the exchange coupling of a dimer of Mn. The spin excitation measured by STM<sup>2</sup> occurs between the antisymmetric spin ground state and the first excited state. These quantum atomic-spin states are not accessible by density-functional electronic-structure calculation. However, the collinear spin states (with parallel and antiparallel spins) of a Heisenberg spin dimer exactly correspond to the collinear magnetic-moment configurations of the real crystal system of the Mn dimer absorbed on the CuN substrate. The parallel and antiparallel spin states have energy expectation values  $\pm JS^2$  respectively. One simply takes the difference of the total energies between the parallel- and antiparallel-spin dimer on the CuN surface, and then extract  $J$  from this energy difference  $\delta E$  and  $S$  by the following equation,

$$\delta E = JS^2 - (-JS^2) = 2JS^2 \quad (1)$$

For a Mn dimer at the Cu site of a CuN surface, we obtain an exchange coupling of  $J = 6.4$  eV from (1), which shows excellent agreement with the STM measured  $J = 6.2 \pm 0.2$  eV. In order to show that this agreement is not just a coincidence, we do the same calculation for a Mn dimer on the N site. The exchange coupling  $J$  turns out to be 2.5 eV, which is also close to the STM measurement ( $J =$

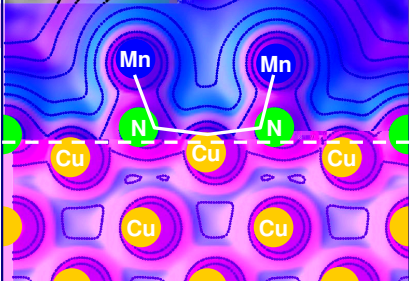


Figure 6: Electron density contour of a Mn dimer at the N site of the CuN surface along the Mn-N row and the out-of-plane direction. The white solid line shows our proposed coupling path between Mn spins. The dashed shows how corrugated the clean CuN surface becomes in the presence of Mn adatoms.

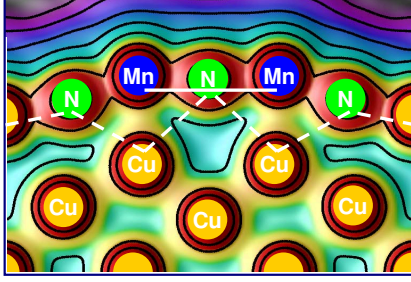


Figure 7: Electron density contour of a Mn dimer at the Cu site of the CuN surface along the N-Mn-N row and the out-of-plane direction. The white solid line shows our proposed coupling path between Mn spins. The dashed shows how corrugated the clean CuN surface becomes in the presence of Mn adatoms.

2.7 eV), and is roughly half of the Cu-site  $J$ . Thus, we have demonstrated that DFT reproduces the exchange coupling between these engineered spins, and will have the capability of predicting similar systems.

In order to check whether it is reasonable to use the  $U$  values determined by the constraint-GGA method in calculating  $J$ , we also calculate  $J$  using other  $U$  values. The resulting  $J$ 's are listed in Table I. We note the significant lack of the agreement of  $J$  calculated by alternative methods with the experimental values. This strongly suggests that the constraint-GGA method can very likely be used to correctly predict the exchange couplings of similar spin systems.

The electron density contour of the N-site Mn dimer in Fig. 6 shows a structure completely different from Mn on the Cu site in Fig. 7. The Mn dimer on the Cu site forms

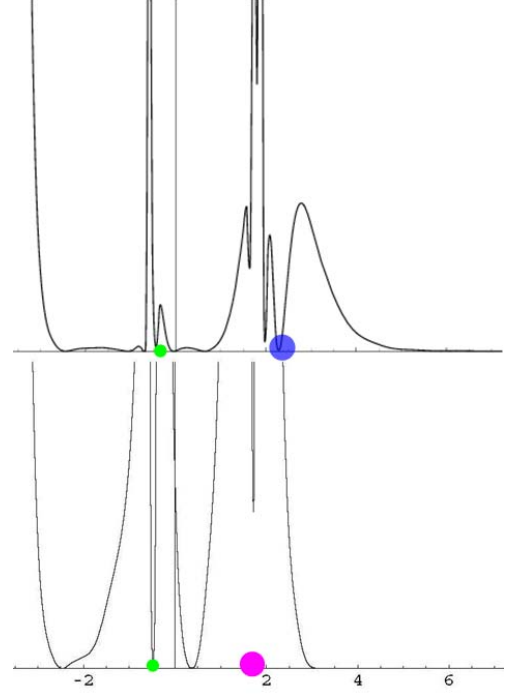


Figure 8: LDOS( $\epsilon_F$ ) along the out-of-surface direction through the adatoms Mn (the larger, solid blue circle in the upper plot) and Co (the larger, solid purple circle in the lower) on the CuN surfaces. The smaller, solid green circles are the Cu atoms underneath the adatoms. The origin is chosen at location of the surface Cu atom of the clean CuN surface, and the vacuum corresponds to positive values of  $z$ .

a chain-like structure bridged by the significantly lifted middle N atom, while on the N site the Mn is attached to the surface like a crown. The binding structures of the Mn atoms strongly suggest that the Mn spins are coupled through the N atoms. The electron density contours indicate that the Mn dimer at the Cu site has a coupling path considerably shorter than when in the surprisingly different structure at the N site. We propose that this explains why the exchange coupling  $J$  measured by STM for the Cu-site Mn dimer has a value twice that of the N-site.

Co atoms on the CuN surface behave quite differently from Mn as experiments<sup>4,5</sup> show. Co displays a Kondo effect, while Mn does not. The relaxed structure via our calculation shows Co settles lower in the surface than Mn (see Fig. 8), and so interacts more with the conduction electrons. We also compare the surface LDOS with Co and Mn as in Fig. 8, and find that there is more LDOS between Co and the Cu underneath it than for Mn. This fact can also be seen by comparing the charge contour plots of these two systems (see Fig.4 and 9). Such substantial LDOS near Co provides the conduction electrons needed for a Kondo effect to happen.

To find the Co spin from our calculation, we plot the

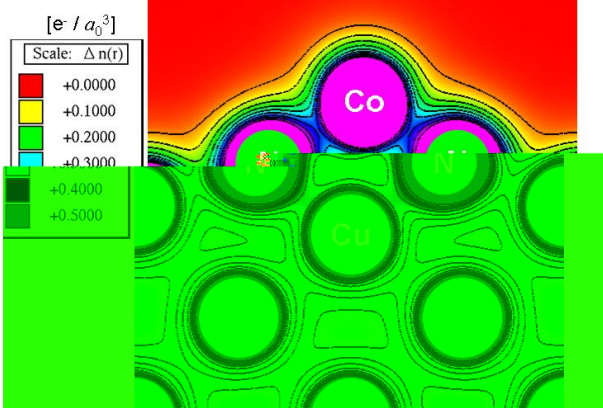


Figure 9: Electron density contour of a single Co on the CuN surface along the N-Co-N row and the out-of-plane direction.

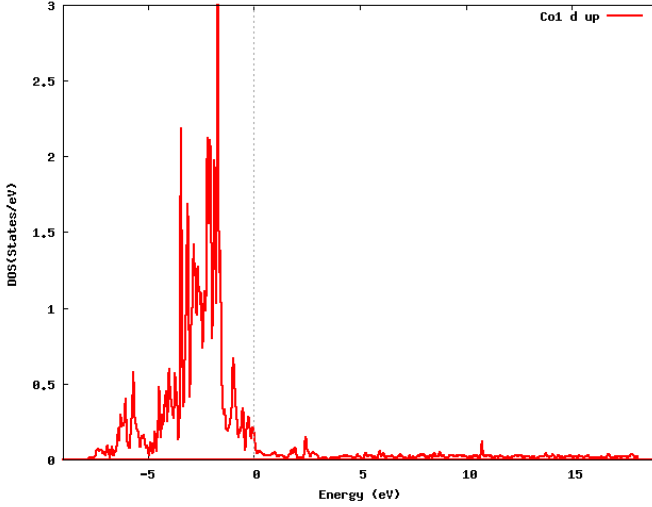


Figure 10: The Co 3d spin-up total density of states on the CuN surface.

densities of states of the 3d Co on the CuN surface as in Fig. 10, 11, and 12. One clearly sees that the spin-up total density of states and the spin-down  $3d_{z^2}$  and  $3d_{x^2-y^2}$  ones are all occupied, while the rest are majority unoccupied. This density-of-state analysis gives  $S = 3/2$  for Co on the CuN surface by approximating the Co 3d in terms of an atomic-like electron configuration of 5 spin-up and 2 spin-down electrons. Another interesting point is to compare the  $U$  values of Co on Au(111) and this CuN/Cu(100) surface since Co/Au(111)<sup>12</sup> is one of the most extensively studied surface Kondo systems. The on-site Coulomb repulsion of Co on Au(111) was extracted to be 2.8 eV from a previous first-principles calculation<sup>13</sup>. The present study has obtained  $U = 0.8$  eV for Co on the CuN surface. The substantial difference of Co  $U$  of the two systems can be explained in the way that Co surrounded by N is more positively charged than that on Cu(111), so adding an electron into Co on CuN is easier

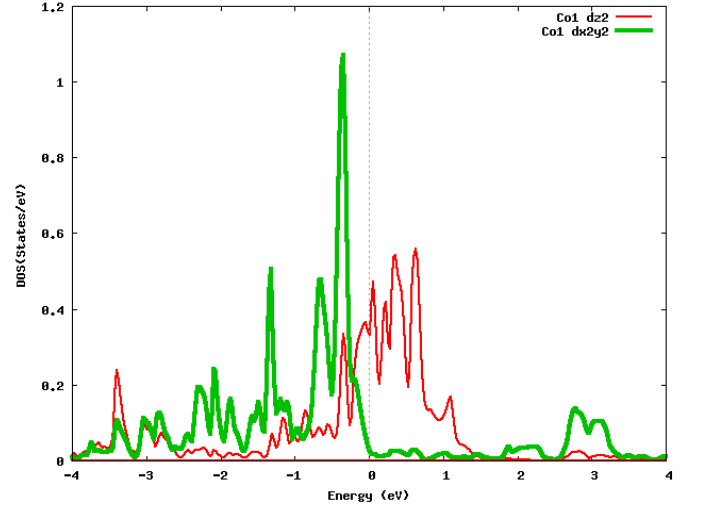


Figure 11: The Co 3d spin-down densities of states of the  $d_{z^2}$  and  $d_{x^2-y^2}$  subshells on the CuN surface.

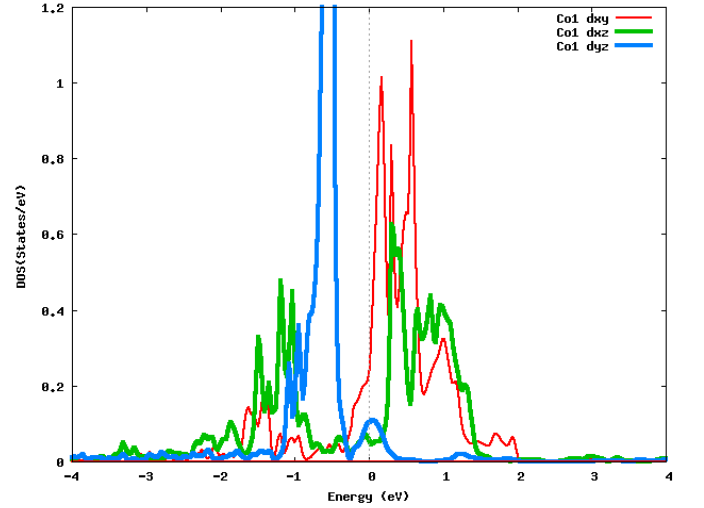


Figure 12: The Co 3d spin-down densities of states of the  $d_{xy}$ ,  $d_{xz}$ , and  $d_{yz}$  subshells on the CuN surface.

because a Co ion attracts an electron more strongly.

#### IV. CONCLUSIONS

In summary, we have calculated the electronic structures of novel engineered spin systems. The precise atomic charges and positions of those systems, not accessible by experimental techniques, are determined by structure relaxation and Bader analysis respectively in our calculations. The charge analysis shows that the Mn-N bond formed by Mn adsorbed on the CuN surface has stronger bond polarity than the Cu-N bond. The presence of Mn gives rise to substantial rearrangement of the

atomic structure: the Mn atoms at the Cu sites perturb their surrounding atomic positions, while those at the N sites do not. The calculated  $J$ 's agree excellently with the STM measurements for two different Mn binding sites. Such agreement serves as a touchstone of DFT's future predictability in similar systems, and is important in searching for a desired  $J$  (e.g. large value or ferromagnetic) for device applications, with the goal of avoiding multiple experimental trials. The electronic structures of the Co atoms on the same surface is also calculated. From that we explain why Co has Kondo effect while Mn doesn't. We also find the Co spin to be  $S = 3/2$ ,

in agreement with the STM's indirect derivation<sup>4</sup>. The on-site Coulomb is calculated to be  $U = 0.8$  eV, much smaller than that of the popular surface Kondo system Co/Au(111), which we explain by the polarities of Co to its nearest neighbor atoms.

We thank C. F. Hirjibehedin, C. P. Lutz, and A. J. Heinrich for stimulating discussions, and the technical help of the IBM Almaden Blue Gene support team. C. Y. Lin acknowledges supports from the Taiwan National Science Foundation, the Taiwan National Center for High-performance Computing, and the Taiwan National Center for Theoretical Sciences (South).

- 
- <sup>1</sup> B. Barbara and L. Gunther, *Physics World* **12**, 35 (1999); D. Gatteschi and R. Sessoli, *Angew. Chem. Int. Ed.* **42**, 268 (2003); M. Verdager, *Polyhedron* **20**, 1115 (2001).
- <sup>2</sup> C. F. Hirjibehedin, C. P. Lutz, and A. J. Heinrich, *Science* **312**, 1021 (2006).
- <sup>3</sup> Some of the results of our work were previously presented in APS March Meeting 2006, which was cited by the paper: A. N. Rudenko *et al.*, *Phys. Rev. B* **79**, 144418 (2009).
- <sup>4</sup> A. F. Otte *et al.*, *Nature Physics*, **4**, 847 (2008).
- <sup>5</sup> A. F. Otte *et al.*, *Phys. Rev. Lett.* **103**, 107203 (2009).
- <sup>6</sup> P. Blaha *et al.*, WIEN2k (Karlheinz Schwarz, Techn. Universität Wien, Austria) (1999), ISBN 3-9501031-1-2.
- <sup>7</sup> J. P. Perdew, K. Burke, and M. Ernzerhof, *Phys. Rev. Lett.* **77**, 3865 (1996).
- <sup>8</sup> G. K. H. Madsen and P. Novák, *Europhys. Lett.* **69**, 777 (2005).
- <sup>9</sup> R. F. W. Bader, *Atoms in Molecules a Quantum Theory*, (Clarendon Press, Oxford, 1994).
- <sup>10</sup> V. I. Anisimov, I. V. Solovyev, M. A. Korotin, M. T. Czyzyk, and G. A. Sawatzky, *Phys. Rev. B* **48**, 16929 (1993);
- <sup>11</sup> A. I. Liechtenstein, V. I. Anisimov, J. Zaanen, *Phys. Rev. B* **52**, R5467 (1995).
- <sup>12</sup> V. Madhavan, W. Chen, T. Jamneala, M. F. Crommie, and N. S. Wingreen, *Science* **280**, 567 (1998).
- <sup>13</sup> O. Újsághy, J. Kroha, L. Szunyogh, and A. Zawadowski, *Phys. Rev. Lett.* **85**, 2557 (2000).